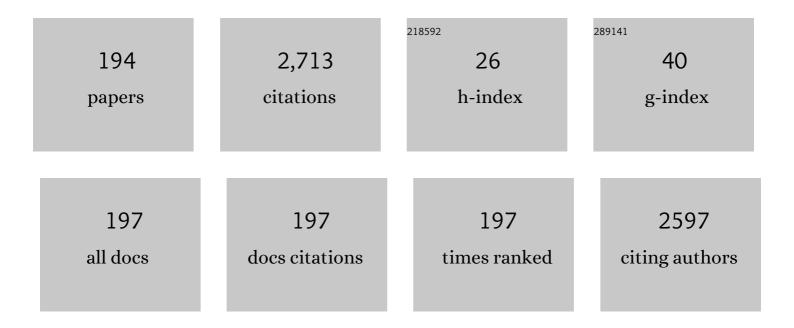
List of Publications by Year in descending order

Source: https://exaly.com/author-pdf/4125642/publications.pdf Version: 2024-02-01



#	Article	IF	CITATIONS
1	In Situ Ambient Pressure XPS Study of CO Oxidation Reaction on Pd(111) Surfaces. Journal of Physical Chemistry C, 2012, 116, 18691-18697.	1.5	135
2	Adsorbate-driven reactive interfacial Pt-NiO _{1â^' <i>x</i>} nanostructure formation on the Pt ₃ Ni(111) alloy surface. Science Advances, 2018, 4, eaat3151.	4.7	76
3	Active Surface Oxygen for Catalytic CO Oxidation on Pd(100) Proceeding under Near Ambient Pressure Conditions. Journal of Physical Chemistry Letters, 2012, 3, 3182-3187.	2.1	67
4	Performance of PF BL-13A, a vacuum ultraviolet and soft X-ray undulator beamline for studying organic thin films adsorbed on surfaces. Journal of Physics: Conference Series, 2013, 425, 152019.	0.3	65
5	Organic matter in extraterrestrial water-bearing salt crystals. Science Advances, 2018, 4, eaao3521.	4.7	64
6	Comparison of the surface electronic structures of H-adsorbed ZnO surfaces: An angle-resolved photoelectron spectroscopy study. Physical Review B, 2011, 83, .	1,1	60
7	Utilizing Carbon Nanotube Electrodes to Improve Charge Injection and Transport in Bis(trifluoromethyl)-dimethyl-rubrene Ambipolar Single Crystal Transistors. ACS Nano, 2013, 7, 10245-10256. Metallization of ampl:math xmlns:mml="http://www.w3.org/1998/Math/MathML"	7.3	56
	display="inline"> <mml:mrow><mml:mtext>ZnO</mml:mtext><mml:mrow><mml:mo>(</mml:mo><ml:mrov< td=""><td>w><mml:mr< td=""><td>ı>10</td></mml:mr<></td></ml:mrov<></mml:mrow></mml:mrow>	w> <mml:mr< td=""><td>ı>10</td></mml:mr<>	ı>10
8	adsorption of hydrogen, methanol, and water: Angle-resolved photoelectron spectroscopy. Physical	1.1	55
9	Review B, 2010, 81, . Control of chemical reactions by core excitations. Journal of Electron Spectroscopy and Related Phenomena, 2001, 119, 255-266.	0.8	50
10	Impact of the molecular quadrupole moment on ionization energy and electron affinity of organic thin films: Experimental determination of electrostatic potential and electronic polarization energies. Physical Review B, 2018, 97, .	1.1	47
11	Development of electron-ion coincidence spectroscopy for the study of surface dynamics combined with synchrotron radiation. Review of Scientific Instruments, 1997, 68, 1703-1707.	0.6	45
12	In situ analysis of catalytically active Pd surfaces for CO oxidation with near ambient pressure XPS. Catalysis Today, 2016, 260, 14-20.	2.2	44
13	Site-specific fragmentation following Si:2p core-level photoionization of F3SiCH2CH2Si(CH3)3 condensed on a Au surface. Journal of Chemical Physics, 1997, 107, 10751-10755.	1.2	41
14	A high-pressure-induced dense CO overlayer on a Pt(111) surface: a chemical analysis using in situ near ambient pressure XPS. Physical Chemistry Chemical Physics, 2014, 16, 23564-23567.	1.3	40
15	Study of ion desorption induced by a resonant core-level excitation of condensed H2O using Auger electron photo-ion coincidence (AEPICO) spectroscopy combined with synchrotron radiation. Surface Science, 1997, 390, 97-101.	0.8	38
16	Full Picture of Valence Band Structure of Rubrene Single Crystals Probed by Angle-Resolved and Excitation-Energy-Dependent Photoelectron Spectroscopy. Applied Physics Express, 2012, 5, 111601.	1,1	37
17	Photostimulated desorption of NO chemisorbed on Pt(100) at 193 nm. Journal of Chemical Physics, 1989, 91, 590-597.	1.2	34
18	Comparison of Solid-Water Partitions of Radiocesium in River Waters in Fukushima and Chernobyl Areas. Scientific Reports, 2017, 7, 12407.	1.6	34

#	Article	IF	CITATIONS
19	<i>In situ</i> removal of carbon contamination from optics in a vacuum ultraviolet and soft X-ray undulator beamline using oxygen activated by zeroth-order synchrotron radiation. Journal of Synchrotron Radiation, 2012, 19, 722-727.	1.0	32
20	lon desorption induced by core-electron transitions studied with electron–ion coincidence spectroscopy. Surface Science, 2000, 451, 143-152.	0.8	31
21	LEED study of NO adsorption-induced restructuring of a single-domain Pt(001)-(20 × 5) surface at 80–410 K. Surface Science, 1992, 277, 97-108.	0.8	29
22	Auger electron photoion coincidence technique combined with synchrotron radiation for the study of the ion desorption mechanism in the region of resonant transitions of condensed H2O. Journal of Chemical Physics, 1998, 108, 6550-6553.	1.2	29
23	Fullerene mixing effect on carrier formation in bulk-hetero organic solar cell. Scientific Reports, 2015, 5, 9483.	1.6	29
24	Photodesorption of NO from Pt(001) at λ=193, 248, and 352 nm. Physical Review B, 1993, 47, 4007-4010.	1.1	28
25	Disappearance of Localized Valence Band Maximum of Ternary Tin Oxide with Pyrochlore Structure, Sn ₂ Nb ₂ O ₇ . Journal of Physical Chemistry C, 2017, 121, 9480-9488.	1.5	27
26	Correlation between Photocatalytic Activity and Carrier Lifetime: Acetic Acid on Single-Crystal Surfaces of Anatase and Rutile TiO ₂ . Journal of Physical Chemistry C, 2018, 122, 9562-9569.	1.5	27
27	In Situ Photoemission Observation of Catalytic CO Oxidation Reaction on Pd(110) under Near-Ambient Pressure Conditions: Evidence for the Langmuir–Hinshelwood Mechanism. Journal of Physical Chemistry C, 2013, 117, 20617-20624.	1.5	26
28	Surface segregation and oxidation of Pt3Ni(1 1 1) alloys under oxygen environment. Catalysis Today, 2016, 260, 3-7.	2.2	26
29	Penning ionization electron spectroscopy of molecules containing the C = O group. Aldehydes and carboxylic acids. The Journal of Physical Chemistry, 1986, 90, 2015-2019.	2.9	25
30	Ion desorption from molecules condensed at low temperature: A study with electron-ion coincidence spectroscopy combined with synchrotron radiation (Review). Low Temperature Physics, 2003, 29, 243-258.	0.2	25
31	High-resolution photoelectron spectroscopy study of degradation of rubber-to-brass adhesion by thermal aging. Applied Surface Science, 2013, 268, 117-123.	3.1	25
32	Operando NAP-XPS Observation and Kinetics Analysis of NO Reduction over Rh(111) Surface: Characterization of Active Surface and Reactive Species. ACS Catalysis, 2018, 8, 11663-11670.	5.5	25
33	A novel organic-rich meteoritic clast from the outer solar system. Scientific Reports, 2019, 9, 3169.	1.6	25
34	Present Status of a New Vacuum Ultraviolet and Soft X-Ray Undulator Beamline BL-13A for the Study of Organic Thin Films Adsorbed on Surfaces. Journal of the Vacuum Society of Japan, 2011, 54, 580-584.	0.3	24
35	Graphene nanoribbons on vicinal SiC surfaces by molecular beam epitaxy. Physical Review B, 2013, 87, .	1.1	24
36	How Rh surface breaks CO2 molecules under ambient pressure. Nature Communications, 2020, 11, 5649.	5.8	24

#	Article	IF	CITATIONS
37	Photostimulated ion desorption from the TiO2(110) and ZnO surfaces. Surface Science, 2004, 572, 43-58.	0.8	23
38	Polarized near-edge x-ray-absorption fine structure spectroscopy of C60-functionalized 11-amino-1-undecane thiol self-assembled monolayer: Molecular orientation and Evidence for C60 aggregation. Journal of Chemical Physics, 2005, 122, 154703.	1.2	23
39	Direct Detection of Fe(II) in Extracellular Polymeric Substances (EPS) at the Mineral-Microbe Interface in Bacterial Pyrite Leaching. Microbes and Environments, 2016, 31, 63-69.	0.7	23
40	Photostimulated desorption of NO on Pt(001) studied with a multiphoton ionization technique. Surface Science, 1991, 242, 444-449.	0.8	22
41	Development of Electron-Ion Coincidence Spectroscopy for the Study of Surface Dynamics. Bulletin of the Chemical Society of Japan, 1996, 69, 1829-1832.	2.0	22
42	Auger-electron-ion coincidence study of photon-stimulated ion desorption for condensed acetonitrile. Surface Science, 1997, 390, 107-111.	0.8	22
43	High-resolution photoelectron spectroscopy analysis of sulfidation of brass at the rubber/brass interface. Applied Surface Science, 2013, 264, 297-304.	3.1	22
44	Determination of the highest occupied molecular orbital energy of pentacene single crystals by ultraviolet photoelectron and photoelectron yield spectroscopies. Japanese Journal of Applied Physics, 2014, 53, 01AD03.	0.8	22
45	Electronic Structures of a Well-Defined Organic Hetero-Interface: C ₆₀ 0n Pentacene Single Crystal. E-Journal of Surface Science and Nanotechnology, 2015, 13, 59-64.	0.1	22
46	Study of ion desorption induced by a resonant core-level excitation of condensed NH3 using Auger-electron photo-ion coincidence (AEPICO) spectroscopy combined with synchrotron radiation. Surface Science, 1997, 390, 102-106.	0.8	20
47	In-situ surface analysis of AuPd(1 1 0) under elevated pressure of CO. Catalysis Today, 2016, 260, 39-45.	2.2	20
48	Site-specific phenomena in Si:2p core-level photoionization of X3Si(CH2)nSi(CH3)3 (X=F or Cl, n=0–2) condensed on a Si(111) surface. Chemical Physics, 1999, 249, 15-27.	0.9	19
49	What Determines the Lifetime of Photoexcited Carriers on TiO ₂ Surfaces?. Journal of Physical Chemistry C, 2016, 120, 29283-29289.	1.5	19
50	High-resolution core-level photoemission measurements on the pentacene single crystal surface assisted by photoconduction. Journal of Physics Condensed Matter, 2016, 28, 094001.	0.7	19
51	Operando Observation of NO Reduction by CO on Ir(111) Surface Using NAP-XPS and Mass Spectrometry: Dominant Reaction Pathway to N ₂ Formation under Near Realistic Conditions. Journal of Physical Chemistry C, 2017, 121, 1763-1769.	1.5	19
52	Two-photon photoemission from NO adsorbed on Cu(111). Surface Science, 1993, 286, 73-81.	0.8	18
53	State-selected ion desorption from condensed H2O at 80 K studied by Auger electron–photoion coincidence spectroscopy. Chemical Physics Letters, 1998, 298, 141-145.	1.2	18
54	Oxygen-free palladium/titanium coating, a novel nonevaporable getter coating with an activation temperature of 133 °C. Journal of Vacuum Science and Technology A: Vacuum, Surfaces and Films, 2018, 36, .	0.9	18

#	Article	IF	CITATIONS
55	Adsorption state selectivity of ultraviolet–laserâ€stimulated desorption of NO chemisorbed on Pt(001) at 80 K studied by (1+1)â€resonanceâ€enhanced multiphoton ionization. Journal of Chemical Physics, 1992, 96, 5523-5528.	1.2	17
56	Site-specific fragmentation caused by core-level photoionization: Effect of chemisorption. Journal of Chemical Physics, 2002, 117, 3961-3971.	1.2	17
57	Electron Donor Molecule on the Oxide Surface: Influence of Surface Termination of ZnO on Adsorption of Tetrathiafulvalene. Journal of Physical Chemistry C, 2011, 115, 21843-21851.	1.5	17
58	Site-Specific Fragmentation following C:1s Core-Level Photoionization of 1,1,1-Trifluoroethane Condensed on a Au Surface and of a 2,2,2-Trifluoroethanol Monolayer Chemisorbed on a Si(100) Surface. Journal of Physical Chemistry B, 2001, 105, 1554-1561.	1.2	16
59	In situ chemical state analysis of buried polymer/metal adhesive interface by hard X-ray photoelectron spectroscopy. Applied Surface Science, 2014, 320, 177-182.	3.1	16
60	Chemical states of surface oxygen during CO oxidation on Pt(1 1 0) surface revealed by ambient pressure XPS. Journal of Physics Condensed Matter, 2017, 29, 464001.	0.7	16
61	Electronic structures and chemical states of methylammonium lead triiodide thin films and the impact of annealing and moisture exposure. Journal of Applied Physics, 2018, 123, .	1.1	16
62	Formation of Carbonate on Ag(111) under Exposure to Ethylene and Oxygen Gases Evidenced by Near Ambient Pressure XPS and NEXAFS. Chemistry Letters, 2019, 48, 159-162.	0.7	16
63	<i>In situ</i> removal of carbon contamination from a chromium-coated mirror: ideal optics to suppress higher-order harmonics in the carbon <i>K</i> edge region. Journal of Synchrotron Radiation, 2015, 22, 1359-1363.	1.0	16
64	LEED observation of NO adsorption-induced relaxation on a single-domain Pt(001)-(20 × 5) surface. Surface Science, 1991, 242, 132-136.	0.8	15
65	Photoelectron spectroscopic study of CO and NO adsorption on Pd(100) surface under ambient pressure conditions. Surface Science, 2013, 615, 33-40.	0.8	15
66	Nanoscale Identification of Extracellular Organic Substances at the Microbe–Mineral Interface by Scanning Transmission X-ray Microscopy. Chemistry Letters, 2015, 44, 91-93.	0.7	15
67	CO Adsorption on Pd–Au Alloy Surface: Reversible Adsorption Site Switching Induced by High-Pressure CO. Journal of Physical Chemistry C, 2016, 120, 416-421.	1.5	15
68	Triangular lattice atomic layer of Sn(1 × 1) at graphene/SiC(0001) interface. Applied Physics Express, 2018, 11, 015202.	1.1	15
69	Heating experiments of the Tagish Lake meteorite: Investigation of the effects of shortâ€ŧerm heating on chondritic organics. Meteoritics and Planetary Science, 2019, 54, 104-125.	0.7	15
70	Development of an electron electron ion coincidence analyzer for Auger photoelectron coincidence spectroscopy (APECS) and electron ion coincidence (EICO) spectroscopy. Journal of Electron Spectroscopy and Related Phenomena, 2007, 161, 164-171.	0.8	14
71	Development of an Apparatus for High-Resolution Auger Photoelectron Coincidence Spectroscopy (APECS) and Electron Ion Coincidence (EICO) Spectroscopy. Journal of the Vacuum Society of Japan, 2008, 51, 749-757.	0.3	14
72	Characterization of Particulate Matters in the Pripyat River in Chernobyl Related to Their Adsorption of Radiocesium with Inhibition Effect by Natural Organic Matter. Chemistry Letters, 2014, 43, 1128-1130.	0.7	14

#	Article	IF	CITATIONS
73	Construction and Evaluation of Coaxially Symmetric Mirror Electron Energy Analyzer with High Sensitivity, and Its Application to Coincidence Spectroscopy. Shinku/Journal of the Vacuum Society of Japan, 2003, 46, 377-384.	0.2	14
74	Angle-Resolved HAXPES Investigation on the Chemical Origin of Adhesion between Natural Rubber and Brass. Langmuir, 2017, 33, 9582-9589.	1.6	13
75	Non-Evaporable Getter (NEG) Coating Using Titanium and Palladium Vacuum Sublimation. Vacuum and Surface Science, 2018, 61, 227-235.	0.0	13
76	Auger electron-ion coincidence study for H2O adsorbed on at 80 K. Surface Science, 1996, 363, 342-346.	0.8	12
77	Auger-final-state selected ion desorption study of condensed NH3 and ND3 by using Auger electron-photoion coincidence spectroscopy. Surface Science, 1997, 377-379, 380-383.	0.8	12
78	Recent progress in coincidence studies on ion desorption induced by core excitation. Journal of Physics Condensed Matter, 2006, 18, S1389-S1408.	0.7	12
79	Surface-site-selective study of valence electronic states of a clean Si(111)-7×7 surface using SiL23VVAuger electron and Si 2pphotoelectron coincidence measurements. Physical Review B, 2011, 83, .	1.1	12
80	High-Pressure NO-Induced Mixed Phase on Rh(111): Chemically Driven Replacement. Journal of Physical Chemistry C, 2015, 119, 3033-3039.	1.5	12
81	Modulation of Electron–Phonon Coupling in One-Dimensionally Nanorippled Graphene on a Macrofacet of 6H-SiC. Nano Letters, 2017, 17, 3527-3532.	4.5	12
82	Construction of a New VUVâ^•Soft X-ray Undulator Beamline BL-13A in the Photon Factory for Study of Organic Thin Films and Biomolecules Adsorbed on Surfaces. AIP Conference Proceedings, 2010, , .	0.3	11
83	Molecular mixing in donor and acceptor domains as investigated by scanning transmission X-ray microscopy. Applied Physics Express, 2014, 7, 052302. A near-ambient-pressure XPS study on catalytic CO oxidation reaction over a Ru(<mml:math) 0="" etqq0="" rgbt<="" td="" tj=""><td>1.1 /Overlock</td><td>11 10 Tf 50 322</td></mml:math)>	1.1 /Overlock	11 10 Tf 50 322
84		0.8	11
85	Surface Science, 2014, 621, 128-132. Anisotropic valence band dispersion of single crystal pentacene as measured by angle-resolved ultraviolet photoelectron spectroscopy. Journal of Materials Research, 2018, 33, 3362-3370.	1.2	11
86	Mechanism of ion desorption induced by core-electron transitions of condensed molecules and adsorbates studied by electron ion coincidence spectroscopy. Journal of Electron Spectroscopy and Related Phenomena, 1999, 101-103, 13-19.	0.8	10
87	Construction and evaluation of an electron-ion coincidence apparatus using a large transmission coaxially symmetric mirror electron energy analyzer. Surface Science, 2003, 528, 261-265.	0.8	10
88	Direct observation of energy band development in a one-dimensional biradical molecular chain by ultraviolet photoemission spectroscopy. Applied Physics Letters, 2013, 102, 134103.	1.5	10
89	A Surface Science Approach to Unveiling the TiO ₂ Photocatalytic Mechanism: Correlation between Photocatalytic Activity and Carrier Lifetime. E-Journal of Surface Science and Nanotechnology, 2019, 17, 130-147.	0.1	10
90	 <i>Operando</i> study of Pd(100) surface during CO oxidation using ambient pressure x-ray photoemission spectroscopy. AIP Advances, 2019, 9, .	0.6	10

#	Article	IF	CITATIONS
91	Enhanced Photoresponsivity of Fullerene in the Presence of Phthalocyanine: A Time-Resolved X-ray Photoelectron Spectroscopy Study of Phthalocyanine/C ₆₀ /TiO ₂ (110). Journal of Physical Chemistry C, 2019, 123, 4388-4395.	1.5	10
92	High sensitivity detection of the frontier electronic states of CH ₃ NH ₃ PbI ₃ single crystals by low energy excitation. Applied Physics Express, 2019, 12, 051009.	1.1	10
93	Study of ion desorption induced by core-level excitations of condensed Si(CH3)4 by using photoelectron-photoion coincidence spectroscopy (PEPICO) combined with synchrotron radiation. Surface Science, 1997, 377-379, 376-379.	0.8	9
94	An Electron-Ion Coincidence Spectroscopy Study of Ion Desorption Induced by Core-Electron Transitions of Surfaces. Japanese Journal of Applied Physics, 1999, 38, 233.	0.8	9
95	Excitation site-specific ion desorption study of Si() surfaces fluorinated by XeF2 using photoelectron photoion coincidence spectroscopy. Surface Science, 2003, 528, 255-260.	0.8	9
96	Construction and Evaluation of Miniature Cylindrical Mirror Electron Energy Analyzer (CMA), and Its Application for Auger-Photoelectron Coincidence Spectroscopy. Shinku/Journal of the Vacuum Society of Japan, 2004, 47, 334-338.	0.2	9
97	Effect of physisorption of inert organic molecules on Au(111) surface electronic states. Physical Chemistry Chemical Physics, 2017, 19, 18646-18651.	1.3	9
98	Electron-Ion Coincidence Spectroscopy as a New Tool for Surface Analysis –an Application to the Ice Surface. Japanese Journal of Applied Physics, 2000, 39, 4489-4492.	0.8	8
99	Development of a miniature double-pass cylindrical mirror electron energy analyzer (DPCMA), and its application to Auger photoelectron coincidence spectroscopy (APECS). Surface Science, 2007, 601, 3589-3592.	0.8	8
100	Auger-electron spectra of F3SiCH2CH2Si(CH3)3 obtained by using monochromatized synchrotron radiation. Journal of Electron Spectroscopy and Related Phenomena, 2009, 175, 14-20.	0.8	8
101	Surface-Site-Selective Study of Valence Electronic Structures of Clean Si(100)-2×1 Using Si-L23VV Auger Electron–Si-2p Photoelectron Coincidence Spectroscopy. Journal of the Physical Society of Japan, 2010, 79, 064714.	0.7	8
102	Topmost-surface-sensitive Si-2p photoelectron spectra of clean Si(100)-2×1 measured with photoelectron Auger coincidence spectroscopy. Surface Science, 2010, 604, L27-L30.	0.8	8
103	Electron-Donor Dye Molecule on ZnO(101Ì0), (0001), and (0001Ì) Studied by Photoelectron Spectroscopy and X-ray Absorption Spectroscopy. Journal of Physical Chemistry C, 2016, 120, 8653-8662.	1.5	8
104	Evidence for chemical bond formation at rubber–brass interface: Photoelectron spectroscopy study of bonding interaction between copper sulfide and model molecules of natural rubber. Surface Science, 2016, 654, 14-19.	0.8	8
105	Improved pumping speeds of oxygen-free palladium/titanium nonevaporable getter coatings and suppression of outgassing by baking under oxygen. Journal of Vacuum Science and Technology A: Vacuum, Surfaces and Films, 2019, 37, .	0.9	8
106	Electronic structure of the clean interface between single crystal CH3NH3PbI3 and an organic hole transporting material spiro-OMeTAD. Applied Physics Letters, 2020, 116, .	1.5	8
107	Twisted bilayer graphene fabricated by direct bonding in a high vacuum. Applied Physics Express, 2020, 13, 075004.	1.1	8
108	Construction and Evaluation of Polar-Angle-Resolved Miniature Time-of-Flight Ion Mass Spectrometer, and Its Application for Electron-Ion Coincidence Spectroscopy. Shinku/Journal of the Vacuum Society of Japan, 2004, 47, 14-21.	0.2	8

#	Article	IF	CITATIONS
109	Effects of the ambient exposure on the electronic states of the clean surface of the pentacene single crystal. Molecular Crystals and Liquid Crystals, 2017, 648, 216-222.	0.4	7
110	Interface Structures and Electronic States of Epitaxial Tetraazanaphthacene on Single-Crystal Pentacene. Materials, 2021, 14, 1088.	1.3	7
111	Miniature Electron/Ion/Soft-X-Ray Detector Mounted on a Conflat Flange with an Outer Diameter of 70 mm. Shinku/Journal of the Vacuum Society of Japan, 2007, 50, 583-585.	0.2	7
112	Quasi-Homoepitaxial Junction of Organic Semiconductors: A Structurally Seamless but Electronically Abrupt Interface between Rubrene and Bis(trifluoromethyl)dimethylrubrene. Journal of Physical Chemistry Letters, 2021, 12, 11430-11437.	2.1	7
113	Competition between Itineracy and Localization of Electrons Doped into the Near-Surface Region of Anatase TiO ₂ . Journal of Physical Chemistry C, 2018, 122, 19661-19669.	1.5	6
114	In-gap state generated by La-on-Sr substitutional defects within the bulk of SrTiO ₃ . Physical Chemistry Chemical Physics, 2019, 21, 14646-14653.	1.3	6
115	XPS study on the thermal stability of oxygen-free Pd/Ti thin film, a new non-evaporable getter (NEG) coating. AIP Conference Proceedings, 2019, , .	0.3	6
116	Operando observations of reactive metal–Oxide structure formation on the Pt3Ni(111) surface at near-ambient pressure. Journal of Electron Spectroscopy and Related Phenomena, 2020, 238, 146857.	0.8	6
117	Orientation-Dependent Hindrance to the Oxidation of Pd–Au Alloy Surfaces. Journal of Physical Chemistry Letters, 2020, 11, 9249-9254.	2.1	6
118	Silicon Single Crystal Wafer Holder with a Cold Trap and a Direct Current Heating Mechanism Mounted on a Conflat Flange with an Outer Diameter of 70 mm. Shinku/Journal of the Vacuum Society of Japan, 2007, 50, 57-59.	0.2	6
119	Beamline commissioning for microscopic measurements with ultraviolet and soft X-ray beam at the upgraded beamline BL-13B of the Photon Factory. Journal of Synchrotron Radiation, 2022, 29, 400-408.	1.0	6
120	Synchrotron Radiation Irradiation Effects forSiHnon Si(100) Surface in the Synchrotron Radiation Stimulated Si Gas Source Molecular Beam Epitaxy. Japanese Journal of Applied Physics, 1995, 34, 6894.	0.8	5
121	Kinetic energy distribution of H+ desorbed by core-level excitations of condensed ammonia using a miniature cylindrical mirror analyzer (CMA). Surface Science, 2005, 593, 291-296.	0.8	5
122	Site-specific ion desorption from condensed F3SiCD2CH2Si(CH3)3 induced by Si-2p core-level ionizations studied with photoelectron photoion coincidence (PEPICO) spectroscopy, Auger photoelectron coincidence spectroscopy (APECS) and Auger electron photoion coincidence (AEPICO) spectroscopy. Surface Science, 2013, 607, 174-180.	0.8	5
123	Photoelectron spectroscopy study of interaction of oxygen with the (111) surface of a Cu–Zn alloy. Surface Science, 2014, 623, 1-5.	0.8	5
124	Shockley surface state on α-brass(111) and its response to oxygen adsorption. Surface Science, 2014, 623, 6-12.	0.8	5
125	Low-cost, high-performance nonevaporable getter pumps using nonevaporable getter pills. Journal of Vacuum Science and Technology A: Vacuum, Surfaces and Films, 2016, 34, .	0.9	5
126	Hydrogen incorporation and release from nonevaporable getter coatings based on oxygen-free Pd/Ti thin films. Journal of Vacuum Science and Technology A: Vacuum, Surfaces and Films, 2019, 37, .	0.9	5

#	Article	IF	CITATIONS
127	Surface analysis and pumping speed measurements of oxygen-free palladium/titanium nonevaporable getter after heating at 100–450 °C. Journal of Vacuum Science and Technology B:Nanotechnology and Microelectronics, 2019, 37, 062923.	0.6	5
128	Development of a high-precision <i>XYZ</i> translator and estimation of beam profile of the vacuum ultraviolet and soft X-ray undulator beamline BL-13B at the Photon Factory. Journal of Synchrotron Radiation, 2020, 27, 923-933.	1.0	5
129	Construction and Evaluation of a Miniature Electron Ion Coincidence Analyzer Mounted on a Conflat Flange with an Outer Diameter of 114 mm. Analytical Sciences, 2008, 24, 87-92.	0.8	4
130	Role of oxygen vacancies in TiO films in electronic structure at interface with an α-NPD layer. Organic Electronics, 2015, 27, 247-252.	1.4	4
131	Catalytic CO oxidation over Pd ₇₀ Au ₃₀ (111) alloy surfaces: spectroscopic evidence for Pd ensemble dependent activity. Chemical Communications, 2017, 53, 12657-12660.	2.2	4
132	Spatially Resolved Distribution of Fe Species around Microbes at the Submicron Scale in Natural Bacteriogenic Iron Oxides. Microbes and Environments, 2017, 32, 283-287.	0.7	4
133	Direct Observations of Correlation between Si-2p Components and Surface States on Si(110)-16 × 2 Single-Domain Surface Using Si-L23VV Auger-Electron and Si-2p Photoelectron Coincidence Measurements. Journal of the Physical Society of Japan, 2017, 86, 054704.	0.7	4
134	Local valence electronic states of silicon (sub)oxides on HfO2/Si-(sub)oxide/Si(110) and HfSi2/Si-(sub)oxide/Si(110) Islands. Surface Science, 2019, 681, 9-17.	0.8	4
135	Initial oxidation of GaAs(100) under near-realistic environments revealed by <i>in situ</i> AP-XPS. Chemical Communications, 2020, 56, 14905-14908.	2.2	4
136	In situ AP-XPS study on reduction of oxidized Rh catalysts under CO exposure and catalytic reaction conditions. Journal Physics D: Applied Physics, 2021, 54, 204005.	1.3	4
137	Formation and Behavior of Carbonates on Ag(110) in the Presence of Ethylene and Oxygen. Journal of Physical Chemistry C, 2021, 125, 9032-9037.	1.5	4
138	Study of Local Valence Electronic States of SiO2Ultrathin Films Grown on Si(111) by Using Auger Photoelectron Coincidence Spectroscopy: Upward Shift of Valence-Band Maximum Depending on the Interface Structure. Journal of the Physical Society of Japan, 2012, 81, 074706.	0.7	4
139	Desorption Induced by Electronic Transitions of Water Adsorbed on Surfaces Shinku/Journal of the Vacuum Society of Japan, 1999, 42, 84-90.	0.2	4
140	Measurements of Ion Kinetic Energy Distribution Using a Miniature Cylindrical Mirror Analyzer (CMA)-Application for H+ Desorption Induced by Core-Level Excitations of Condensed Water. Shinku/Journal of the Vacuum Society of Japan, 2005, 48, 286-289.	0.2	4
141	Titanium Dioxide (TiO2) Single Crystal Holder with a Cold Trap and a Heating Mechanism Mounted on a Conflat Flange with an Outer Diameter of 70 mm. Journal of the Vacuum Society of Japan, 2008, 51, 44-47.	0.3	4
142	Development of One-Body Type Water- and Air-Cooling Fixed Masks Made of Forged 0.2% Beryllium Copper Alloy. Journal of the Vacuum Society of Japan, 2010, 53, 454-457.	0.3	4
143	Ultra fast H ⁺ Desorption from an Isolated NH ₃ Monolayer Adsorbed on a Xe Film Induced by a Resonant Core Electron Transition Studied by Auger Electron-Photoion Coincidence Spectroscopy. Japanese Journal of Applied Physics, 1999, 38, 325.	0.8	4
144	Construction and Evaluation of Retractable Auger Electron Spectrometer with an Electron Gun Mounted on a Conflat Flange with an Outer Diameter of 70 mm. Shinku/Journal of the Vacuum Society of Japan. 2005. 48. 552-556.	0.2	4

#	Article	IF	CITATIONS
145	Ion desorption caused by N1s core-level photoexcitation of N2O on Si(100) surface. Surface Science, 2005, 593, 276-282.	0.8	3
146	Construction of Simple Non-Evaporable Getter Assemblies Using St707 Strips. Journal of the Vacuum Society of Japan, 2010, 53, 533-534.	0.3	3
147	Ion Desorption from Single-Walled Carbon Nanotubes Induced by Soft X-ray Illumination. Japanese Journal of Applied Physics, 2010, 49, 105104.	0.8	3
148	Local Valence Electronic States of SiO2 Ultrathin Films Grown on Si(100) Studied Using Auger Photoelectron Coincidence Spectroscopy: Observation of Upward Shift of Valence-Band Maximum as a Function of SiO2 Thickness. Journal of the Physical Society of Japan, 2011, 80, 084703.	0.7	3
149	Development of low-cost, high-performance non-evaporable getter (NEG) pumps. AIP Conference Proceedings, 2016, , .	0.3	3
150	Element selective oxidation on Rh–Pd bimetallic alloy surfaces. Physical Chemistry Chemical Physics, 2018, 20, 28419-28424.	1.3	3
151	Development of a new NEG pump using oxygen-free Pd/Ti thin film. AIP Conference Proceedings, 2019, , .	0.3	3
152	Electronic structure of <mml:math xmlns:mml="http://www.w3.org/1998/Math/MathML"><mml:msup><mml:mn>3</mml:mn><mml:mo>â~-twisted bilayer graphene on 4H-SiC(0001). Physical Review Materials, 2021, 5, .</mml:mo></mml:msup></mml:math 	nl:m@.9/mr	nl:n a sup>
153	Report on Water-Cooled Movable Masks Made of Forged 0.2% Beryllium Copper Alloy. Journal of the Vacuum Society of Japan, 2011, 54, 481-482.	0.3	3
154	Ligand effects on surface oxide at RhPd(100) alloy surfaces: A density functional theory calculation study. Surface Science, 2022, 716, 121958.	0.8	3
155	Elaboration of nearâ€valence band defect states leading deterioration of ambipolar operation in SnO thinâ€film transistors. Nano Select, 2022, 3, 1012-1020.	1.9	3
156	Structure and Photo-Induced Charge Transfer of Pyridine Molecules Adsorbed on TiO2(110): A NEXAFS and Core-Hole-Clock Study. Electrochemistry, 2014, 82, 341-345.	0.6	2
157	Decay Processes of Si 2sCore Holes in Si(111)-7 × 7 Revealed by Si Auger Electron Si 2sPhotoelectron Coincidence Measurements. Journal of the Physical Society of Japan, 2014, 83, 094704.	0.7	2
158	Structure and electronic structure of van der Waals interfaces at a Au(1 1 1) surface covered with a well-ordered molecular layer of n-alkanes. Applied Surface Science, 2021, 535, 147673.	3.1	2
159	Simple Evaporator for Metal Evaporation Mounted on a Conflat Flange with an Outer Diameter of 70 mm. Journal of the Vacuum Society of Japan, 2008, 51, 99-101.	0.3	2
160	A newly designed compact CEY-XAFS cell in the soft X-ray region and its application to surface XAFS measurements under ambient-pressure conditions without photoinduced side effects. Physical Chemistry Chemical Physics, 2022, 24, 2988-2996.	1.3	2
161	Construction of Simple Non-Evaporable Getter Assemblies Using St 707 Strips or St 172 Modules. Journal of the Vacuum Society of Japan, 2012, 55, 21-23.	0.3	1
162	Publisher's Note: Graphene nanoribbons on vicinal SiC surfaces by molecular beam epitaxy [Phys. Rev. B87, 121407(R) (2013)]. Physical Review B, 2013, 87, .	1.1	1

#	Article	IF	CITATIONS
163	What Does the Angle-Integrated Photoelectron Spectrum Show? A Comparison between First-Principles Calculation and Experiments for Graphite. Journal of the Physical Society of Japan, 2014, 83, 084705.	0.7	1
164	Influence of Stacking Order of Phthalocyanine and Fullerene Layers on the Photoexcited Carrier Dynamics in Model Organic Solar Cell. Journal of Physical Chemistry C, 2021, 125, 13963-13970.	1.5	1
165	Simultaneous Measurements of Mass and Kinetic-Energy Distribution of Ions Using a Miniature Cylindrical Mirror Analyzer (CMA) and Synchrotron Radiation under the Single-Bunch Mode Operation-Application for H+ Desorption Induced by Core-Level Excitations of Condensed Ammonia Shinku/Iournal of the Vacuum Society of Japan. 2007, 50, 530-533.	0.2	1
166	Damage at KEK B Factory and Photon Factory due to the Great East Japan Earthquake. Journal of the Vacuum Society of Japan, 2012, 55, 7-10.	0.3	1
167	Pioneers of Study on Desorption Induced by Electronic Transitions; Achievements by Dr. Yoshioki Ishikawa and Dr. Yoshio Ohta. Shinku/Journal of the Vacuum Society of Japan, 2006, 49, 610-617.	0.2	1
168	Simple Low-Outgassing Atomic Hydrogen Source. Journal of the Vacuum Society of Japan, 2012, 55, 403-404.	0.3	1
169	Report on the School Course Held in the Joint Annual Symposium of the Vacuum Society of Japan and the Surface Science Society of Japan (SVSS'13). Journal of the Vacuum Society of Japan, 2014, 57, 202-203.	0.3	1
170	Ion Desorption by Inner-shell Excitation and Photodegradation of Poly(vinylidene fluoride). Materials Research Society Symposia Proceedings, 2005, 887, 1.	0.1	0
171	Development of a compact electron ion coincidence analyzer using a coaxially symmetric mirror electron energy analyzer and a miniature polar-angle-resolved time-of-flight ion mass spectrometer with four concentric anodes. Review of Scientific Instruments, 2009, 80, 043303.	0.6	0
172	Hydrogen ion desorption from amorphous carbon films induced by resonant core electron excitations. Nuclear Instruments & Methods in Physics Research B, 2010, 268, 127-130.	0.6	0
173	Auger electron spectra of hydrogenated Si(111)-1×1 surface obtained from <i>Si-L</i> ₂₃ <i>VV</i> Auger electron Si-2 <i>p</i> photoelectron coincidence measurements. Journal of Physics: Conference Series, 2011, 288, 012016.	0.3	0
174	Local Valence Electronic States and Valence-Band Maximum of Ultrathin Silicon Nitride Films on Si(111) Studied by Auger Photoelectron Coincidence Spectroscopy: Thickness and Interface Structure Dependence. Journal of the Physical Society of Japan, 2015, 84, 044711.	0.7	0
175	Report on the School Course Held in the 55th Annual Symposium of the Vacuum Society of Japan. Journal of the Vacuum Society of Japan, 2015, 58, 162-163.	0.3	0
176	Report on the Japan Vacuum Show "VACUUM2014". Journal of the Vacuum Society of Japan, 2015, 58, 190-192.	0.3	0
177	Morphology of F8T2/PC71BM Blend Film as Investigated by Scanning Transmission X-ray Microscope (STXM). Molecular Crystals and Liquid Crystals, 2015, 620, 32-37.	0.4	0
178	Report of 1st Vacuum Technology Course for Non-Specialists. Journal of the Vacuum Society of Japan, 2016, 59, 251-252.	0.3	0
179	Construction of a Simple Metal Evaporator Mounted on a Conflat Flange with an Outer Diameter of 70 mm. Journal of the Vacuum Society of Japan, 2016, 59, 138-140.	0.3	0
180	Report on the Japan Vacuum Show "VACUUM2015". Journal of the Vacuum Society of Japan, 2016, 59, 141-143.	0.3	0

#	Article	IF	CITATIONS
181	Two-dimensional Electron Gas at Thiol/ZnO Interface. E-Journal of Surface Science and Nanotechnology, 2020, 18, 41-47.	0.1	0
182	Studies on the Core-level-excitation-induced Ion Desorption from Solid Surfaces Hyomen Kagaku, 2002, 23, 753-758.	0.0	0
183	Report on the 29th Japan Vacuum Show "VACUUM2007â€: Shinku/Journal of the Vacuum Society of Japan, 2007, 50, 688-692.	0.2	Ο
184	Report on Construction of Digital Archive of "Shinku―and Publication of Electronic Journal. Journal of the Vacuum Society of Japan, 2009, 52, 30.	0.3	0
185	Report on the 30th Japan Vacuum Show "VACUUM2008― Journal of the Vacuum Society of Japan, 2009, 52, 12-16.	0.3	0
186	Report on the 32nd Japan Vacuum Show "VACUUM2010― Journal of the Vacuum Society of Japan, 2011, 54, 67-71.	0.3	0
187	Report on the Japan Vacuum Show "VACUUM2011â€. Journal of the Vacuum Society of Japan, 2012, 55, 129-130.	0.3	0
188	Electronic Structure of Organic Biradical Molecular Films. Journal of the Vacuum Society of Japan, 2013, 56, 32-38.	0.3	0
189	Report on the Symposium ^ ^ldquo;New Aspects of Materials Science Pioneered by Neutron and Muon Beams^ ^rdquo; Planned by the Vacuum Society of Japan. Journal of the Vacuum Society of Japan, 2013, 56, 280-282.	0.3	0
190	Report on the Japan Vacuum Show ^ ^ldquo;VACUUM2012^ ^rdquo;. Journal of the Vacuum Society of Japan, 2013, 56, 107-110.	0.3	0
191	Attempts to Improve the Sensitivity and the Energy Resolution of an Analyzer for Auger Photoelectron Coincidence Spectroscopy and Electron Ion Coincidence Spectroscopy. Journal of the Vacuum Society of Japan, 2013, 56, 507-510.	0.3	0
192	Photostimulated Desorption of NO Chemisorbed on Pt (001) at 193 nm. Progress of Theoretical Physics Supplement, 2013, 106, 349-359.	0.2	0
193	Report on the Japan Vacuum Show ^ ^ldquo;VACUUM2013^ ^rdquo;. Journal of the Vacuum Society of Japan, 2014, 57, 117-120.	0.3	0
194	In situ observation of surface reactions with synchrotron radiation induced semiconductor processes by infrared reflection absorption spectroscopy using buried metal layer substrates. IEEJ Transactions on Electronics, Information and Systems, 1996, 116, 1348-1355.	0.1	0